Electric Power Systems Research 202 (2022) 107602

Contents lists available at ScienceDirect

Electric Power Systems Research

journal homepage: www.elsevier.com/locate/epsr

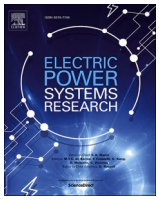

Fuzzy based relaying scheme for high impedance faults in DG integrated distribution system

Maanvi Bhatnagar [a], Anamika Yadav [a,*], Aleena Swetapadma [b]

[a] Department of Electrical Engineering, National Institute of Technology Raipur, 492010, India
[b] School of Computer Engineering, KIIT Deemed to be University, Bhubaneswar 751024, India

ARTICLE INFO

Keywords:
Distribution lines
HIF
Fault detection
Fault classification
Fuzzy inference system

ABSTRACT

Most of the high impedance faults (HIF) remain un-detected by the conventional relays due to non-linear nature of the fault and low magnitude of current. In this work, a combination of discrete wavelet transforms (DWT) and fuzzy inference system (FIS) has been proposed for HIF detection and classification. Modified IEEE 13 node test feeder system has been to validate the proposed scheme. The proposed method uses current signals from one end that are pre-processed using discrete wavelet transform to obtain appropriate input features. The wavelet processed features are given to the FIS for fault detection and classification. Proposed method has been validated using both Mamdani and Sugeno type FIS. Different operating and fault conditions are tested to validate the proposed method such as varying DG parameters, noisy signals, HIFs, evolving faults, fault inception angle, fault resistance, fault location, and non-fault events (e.g. motor load switching, capacitor switching, DG switching, transformer energization, non-linear load switching). The accuracy in detecting and classifying the faults is 100% of all the tested fault cases. Results shows that the overall detection time required to detect the HIFs is minimum 4.25 cycles in most of the cases and maximum 8 cycles in few cases whereas for shunt faults is within 4.25 to 6 cycles only. Advantage of the proposed method is that it can detect adverse situation faults like evolving faults, in presence of noisy signals and remains intact against any switching events. The results of the proposed method are promising and the method is robust against various operating conditions.

1. Introduction

Detection of HIFs has always posed as a critical problem for utilities and researchers since many years especially in the power distribution systems. This type of fault is ensued whenever a primary feeder energized conductor comes in contact either with the ground or some other poorly grounded object such as wooden fences, trees or vehicles. Also, at times the conductor breakdown and comes in contact with surface offering very high impedance for instance grass, concrete, sand asphalt etc. This results in very low magnitude fault current ranging between a few mA up to 100 A [1]. Due to such low magnitude of fault current, HIFs do not pose to be a threat for operation of power distribution system network. But such faults can prove to be fatal for the general public because if a person comes in contact with these live open conductors, he may get an electric shock. If these faults are not cleared on time, they can be hazardous for public and property. These faults are difficult to detect by using simple protection schemes such as fuses and overcurrent relays because of low magnitude of fault currents. A shunt fault can easily be detected in 1-2 cycles after its occurrence but an HIF can go un-detected for up to a few hours. Also, if there are distributed generators (DGs) attached to the network then the detection of HIFs becomes even more cumbersome [2]. The distribution system is no more radial after incorporation of DG. So, the conventional overcurrent relay experiences loss of coordination. Furthermore, the contribution in fault current from DGs is dependent upon the type of DG employed in the system. For instance, for an inverter-based DG the fault current is limited whereas in a synchronous generator DG the contribution in fault current is high. Because of the variable contribution in the fault current from different DGs in the downstream, the relays located in upstream substation get blinded. This leads to delayed or false tripping of the relay, making the process of HIF detection difficult. Despite these challenges the researchers are optimistic towards finding efficient HIF fault detection methodologies.

Various schemes have been already reported in the literature in the past. In [3], state estimation algorithm has been augmented which allows fault detection across the network on IEEE 13 bus and 123 bus systems. In [4], a physics based analytical model for fault estimation in

* Corresponding author.
E-mail addresses: ayadav.ele@nitrr.ac.in, anamikajugnu4@gmail.com (A. Yadav).

https://doi.org/10.1016/j.epsr.2021.107602
Received 21 June 2021; Received in revised form 1 September 2021; Accepted 16 September 2021
Available online 27 September 2021

Nomenclature

AI	artificial intelligence
BESS	battery energy storage system
DGs	distributed generators
DWT	discrete wavelet transforms
EMD	empirical mode decomposition
EVF	evolving fault
FIS	fuzzy inference system
HIF	high impedance fault
HHT	Hilbert Huang transform
LSW	load switching
LIF	low impedance fault
SNR	signal to noise ratio
SVM	support vector machine
VMD	variational mode decomposition

distribution systems has been introduced. Most of the reported techniques makes use of time-domain, frequency domain or time scale domain analysis [5]. In [6], a real-time fault detection and faulted line identification functionality obtained by computing parallel synchrophasor-based state estimators. In [7], a window based short time Fourier transform (STFT) technique is proposed which is based on frequency domain analysis. Fuzzy based techniques are also being popularly used for fault classification because of their capability to deal with uncertain fault data [8].

DGs are being popularly used in the modern era power distribution networks and therefore their effect on overall system operation is a matter of great concern. The fault current is dependent on the type of DG added in the system for instance high fault current is observed in case of synchro-generator DG whereas an inverter-based DG limits the fault current magnitude [9]. In [10], an intrinsic time decomposition and Teager Kaiser energy operator (TKEO) which detects the fault based on comparison with threshold values has been reported. In [11], a scheme using weighted least square approach has been testified but does describe about non-faulty events such as switching. An innovative HIF identification method using TKEO and variational mode decomposition (VMD) scheme which is immune to noise and also identifies faulty and non-faulty events has been described in [12]. HIF distance is estimated through a weighted least squares estimator associated with a parametric error processing algorithm in [13]. In [14], a fast directional detection of phase-to-ground faults in isolated neutral distribution grids has been proposed. A searching-based method for locating high impedance arcing fault in distribution network has been proposed in [15]. In [16], a transient-based algorithm for high-impedance fault identification on distribution networks using discrete wavelet transform has been proposed.

Artificial intelligence (AI) based method are also applied by researchers for detecting HIF in distribution systems. In [17], HIF detection using the help of discrete wavelet transforms with evolving neural network technique has been suggested. A support vector machine (SVM) and time-frequency analysis scheme for fault detection in distribution system has been reported in [18]. Another wavelet transform and evolving neuro fuzzy technique is reported in [19]. In [20], a hybrid scheme using VMD and SVM for detecting and classifying faults in modified IEEE 13 bus system has been proposed. Hilbert Huang transform (HHT) for feature extraction and machine learning model has been used for HIF detection in [21]. HHT makes use of empirical mode decomposition (EMD) method for the purpose of feature extraction but has certain restrictions such as sensitivity towards noise and mode mixing. In [22], a neural network-based method for non-linear high impedance fault distance estimation in power distribution systems has been proposed. But drawback of AI-based method is that it requires a large data set for training of the machine learning model, which is quite cumbersome task, also tuning of the parameters of AI-based scheme is complex task.

The shortcomings of the prevailing conventional protection schemes are as follows:-

- The incapability of conventional protection scheme to detect the high impedance faults, faults during change in DG parameters.
- Mal-operation of conventional protection scheme during various switching events such as non-linear load switching, DG switching, transformer energization, capacitor switching etc. These events are considered as fault events by conventional relay.

These shortcomings are addressed in the proposed DWT-Fuzzy

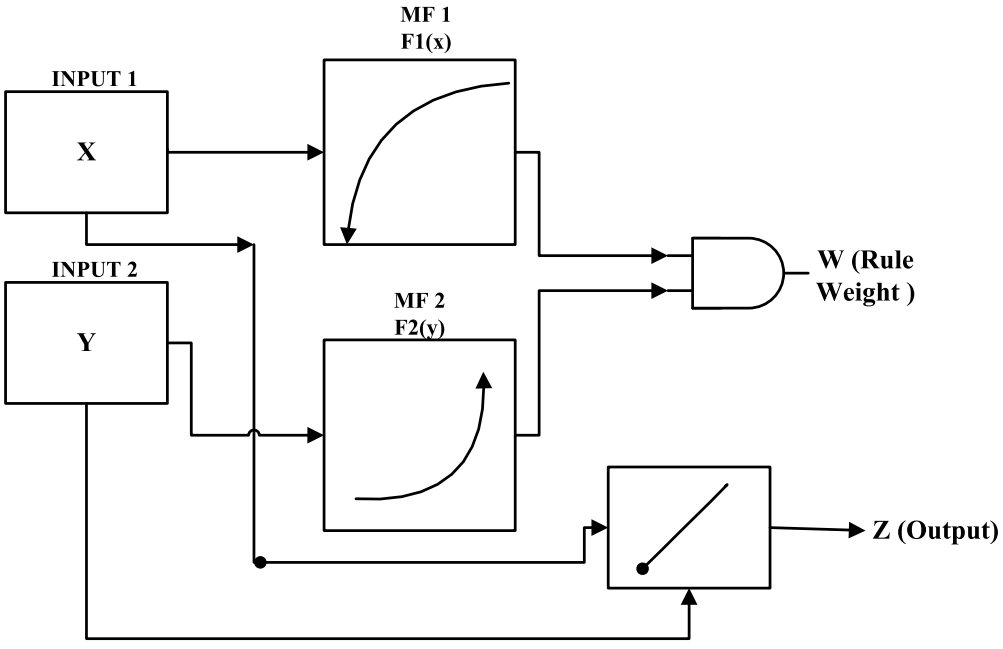

Fig. 1. Operation of rules in Sugeno system for a set of two inputs.

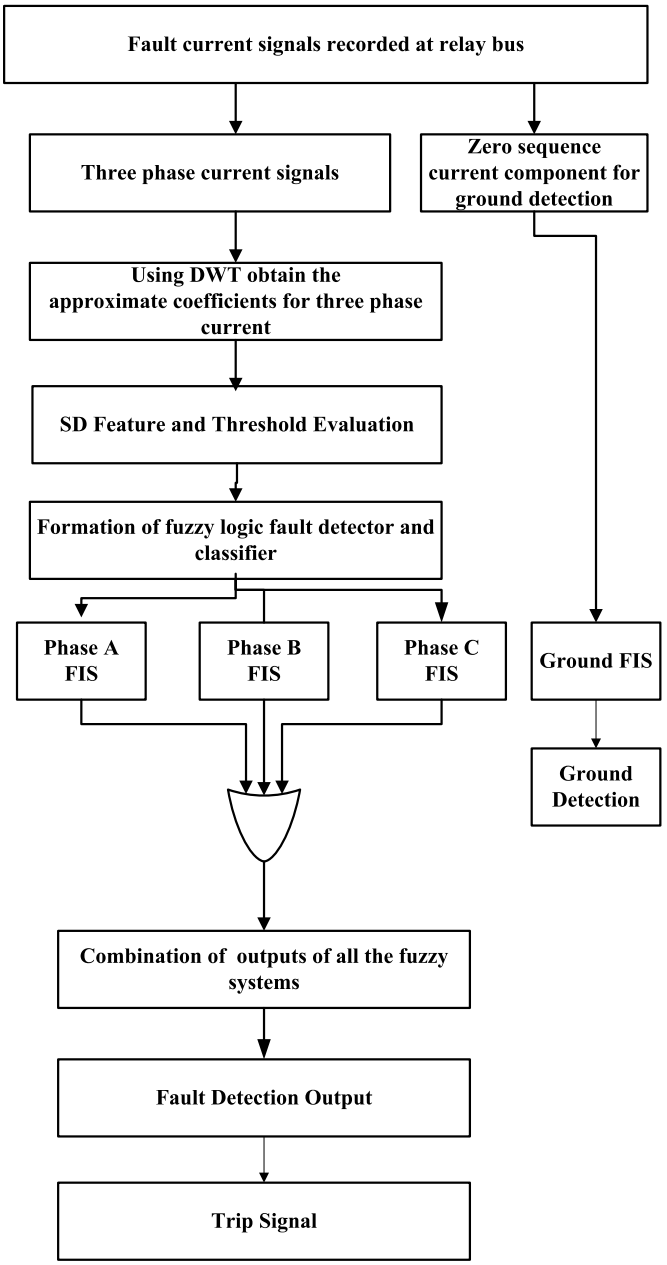

Fig. 2. Flowchart representing the proposed methodology for fault detection scheme.

method. Additionally, the proposed scheme also takes into account the evolving faults and effect of noise. There are many papers involving use of wavelet transform and soft computing techniques such as ANN, SVM, DT for classification/decision criteria but there are very few papers [8, 19] reported in literature which uses fuzzy inference system along with wavelet transform [19] for HIF. Another paper is reported in [8] which use harmonic current as input to fuzzy logic-based scheme for HIF detection. But these papers have not considered the impact of EVF, non-linear load switching and DGs integration etc. In this paper, at relaying bus, the fault current signals are acquired and DWT is used for computation of features. DWT being a time-frequency approach is insensitive to noise. DWT is used to calculate the first level approximate wavelet coefficients. With the help of a moving window, standard deviation (SD) of first level approximate wavelet coefficients of three phase fault currents for each passing window has been computed. These SD values of three phase fault currents are then used for designing of fuzzy inference system for each phase whose combined output gives the information of fault detection and classification. The paper is organized in the following manner Section 2 gives detail about the FIS, Section 3 discusses about the proposed scheme, Section 4 elaborates the results and discussion, Section 5 carries out a comparative assessment and finally Section 6 concludes of the paper.

2. Techniques used

2.1. Fuzzy inference systems

In the modern era power system protection, application of fuzzy logic-based techniques has increased many folds. These systems are easily comprehensible, flexible in nature, tolerant to vague data and most importantly offer tradeoff between precision and significance. To develop a fuzzy inference system, the steps involved are fuzzification, application of fuzzy operator, application of implication method, aggregation of all outputs, and defuzzification [23]. Two different types of fuzzy inference systems can be built namely Mamdani FIS and Sugeno FIS using membership functions such as sigmoidal, triangular, trapezoidal and Gaussian can be used to design the FIS.

In Mamdani system, the output obtained corresponding to each rule is a fuzzy set. A Sugeno inference system has singleton output membership functions. These can be linear or constant in nature depending on the type of input value. Output of rule can be constant or a linear function of input. It is defined as:

$$z_j = a_j x + b_j y + c_j \tag{1}$$

a_j, b_j, c_j are constant coefficients. Similarly, w (weight of rule) is defined as

$$w_i = \text{AndMethod}(F1(x), F2(y)) \tag{2}$$

Where $F1(x)$ and $F2(y)$ are the input membership functions. The rules of Sugeno FIS operate as illustrated in Fig. 1. Fig. 1 shows two values are being generated for each rule, z (output of rule) and w (weight of rule). The final output is given by the weighted average of all the output rules. It can be shown mathematically as:

$$\text{Output} = \frac{\sum_{j=1}^{K} w_j z_j}{\sum_{j=1}^{K} w_j} \tag{3}$$

Here K is the total number of rules. With the help of all the steps discussed above, both Mamdani and Sugeno FIS for fault detection and classification has been designed which will be discussed in next section.

2.2. Discrete wavelet transform

DWT is efficient in processing signal features that are localized in both frequency and time. The signals can be decomposed using DWT with the help of Eq. (4) given as [26]:

$$\text{DWT}(S(e,f)) = \frac{1}{\sqrt{a_o^f}} \sum_m s(m) \phi^* \left(\frac{f - m b_o a_o^e}{a_o^e} \right) \tag{4}$$

where a_o and b_o are the parameters of scaling and shifting, respectively, ϕ^* represents mother wavelets conjugate. Out of different type of mother wavelet, db wavelet is more prominently used in power system signal analysis [27]. The Daubechies family of wavelets are a type of compactly supported orthogonal wavelets which makes them suitable for discrete wavelet analysis. These wavelets are recognized by the maximum number of vanishing moments for a given support width. There is a scaling function for every type of wavelet belonging to this class known as the mother wavelet which produces an orthonormal multiresolution analysis. The scaling filters associated are minimum phase filters. This wavelet family have extremal phase and are written as db$N$ for $N = 1, 2 \ldots 45$. Here db corresponds to the wavelets surname and N represents

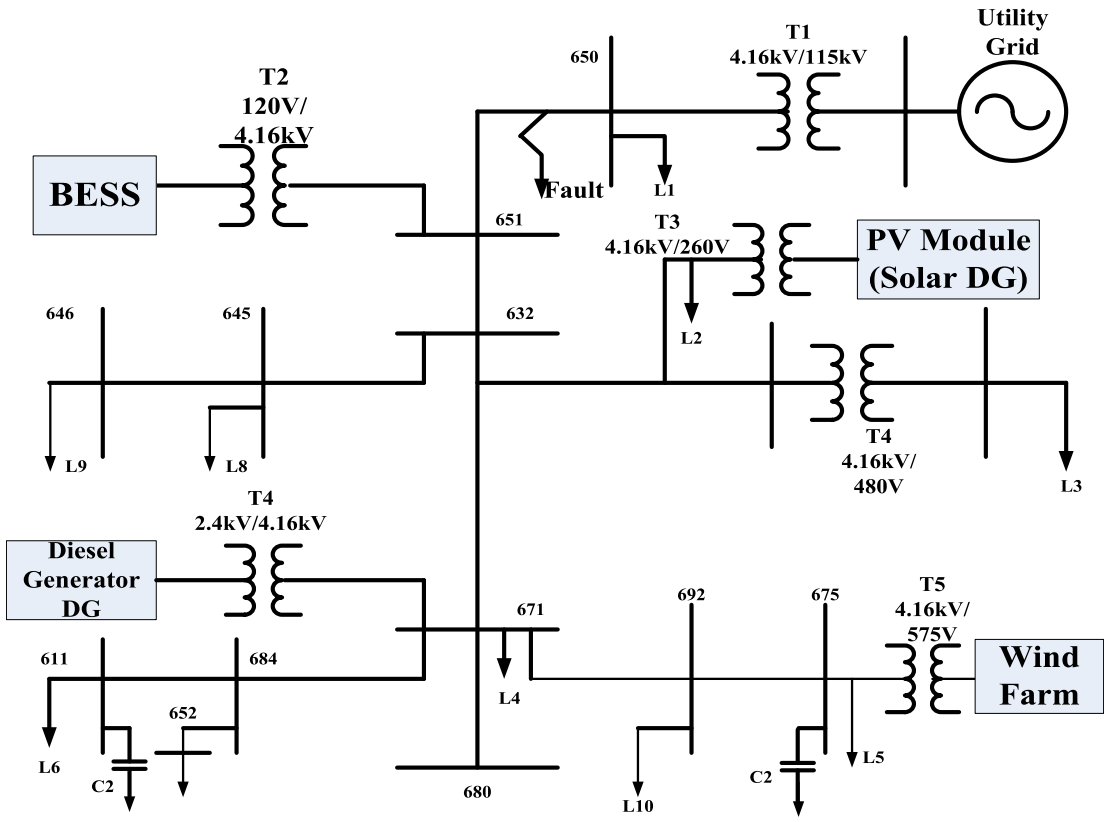

Fig. 3. Single line diagram of modified IEEE-13 bus test node feeder.

the number of vanishing moments. The role of vanishing moments is to limit the ability of wavelet to characterize behavior of a polynomial or signal information. The db1 or the Daubechies 1 wavelet is the simplest, fastest and most memory efficient type of wavelet belonging to this family. It has one vanishing moment and can easily translate polynomials having one coefficient. Wavelet 'db1' is discontinuous in nature and looks like a step function. In this work 'db1' wavelet has been used to processes the signal.

3. Proposed method

Proposed DWT and FIS based method detects the HIF as well as low impedance faults (LIF). Details of the proposed method have been shown in Fig. 2 and described in the sub-sections hereunder.

3.1. Input test system

The single line diagram of IEEE-13 bus distribution system has been shown in Fig. 3 [24] which is used for case studies in this work. This is a modified version of the standard system and consists of four DG units namely solar (0.3 MW), wind (1.5 MW), diesel generator DG (3.125 MVA) and battery-based energy storage (BESS) (200 kWh). Details of modifications made to the IEEE 13 bus test system to use the Matlab/-Simulink models are given in the Appendix A. The irradiance operational condition for solar DG is $I = 1000\ \frac{W}{m^2}$. The wind speed operational condition for wind DG is ώ = 15 m/s. The main utility grid feeds the entire system and has 1000 MVA short circuit rating and operates at 120 kV and 60 Hz. The test system has three-phase, two-phase and single-phase pi section lines connected with various types of loads at, respective buses. Bus number 650 is taken as the relaying bus and all the current measurements are done at this bus. The system frequency is 60 Hz and the sampling frequency is 1.2 kHz. The power flow is from the utility grid towards the rest of test system. The system is modelled using MATLAB/SIMULINK as shown in Fig. 3 [25].

HIF faults occur when a live conductor touches a surface which offers high impedance. To replicate a real HIF fault model that exhibits typical HIF characteristics such as asymmetry, nonlinearity, build-up, shoulder, intermittence and randomness has been shown in Fig. 4. It consists of two anti-parallel diodes, two variable resistances R_p, R_n and two dc voltage sources V_p, V_n for every phase. For imitating a real time model of fault occurring on concrete surface of 10 cm thickness the parameters are chosen as $V_n = 1700V, V_p = 400V, R_p, R_n$ are varied between 40Ω – 150Ω in the steps of 10Ω. The resistances are varied arbitrarily every half-cycle, meaning that the resistance value keeps increasing and decreasing in every alternate half cycle [20].

3.2. Signal processing and input feature extraction

To capture the slow oscillations occurring in HIF current signals, DWT has been utilized as the feature extraction method. In this work, DWT is used to process the current signals and find the appropriate input features for detection and classification of fault. From the family of Daubechies wavelet, 'db1' wavelet has been chosen for wavelet decomposition. To extract input features, first level approximate coefficients are obtained after decomposing the current signals of each phase using db1 wavelet with the help of a short recursive moving window of one cycle. The standard deviation feature of approximate coefficients of level 1 is calculated. Then the window keeps moving forward through each data points till the end of the simulation time to obtain the input features in time domain. Fig. 5 shows the signal processing and feature extraction used to find the input current feature. First plot of Fig. 5 shows the phase current during ACG-HIF at 0.033 s with moving windows such as window 1(sample number 1–20), window 2 (sample number 2–21) and window 3 (sample number 2–22). Second plot of Fig. 5 shows one cycle samples of window 1 that is taken for processing with DWT. Third plot of Fig. 5 shows the approximate

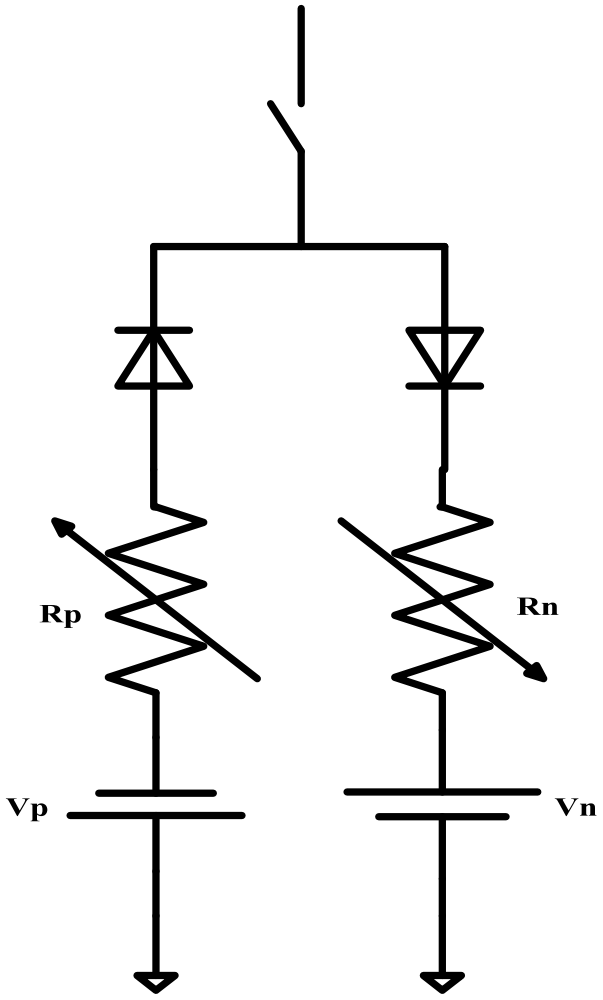

Fig. 4. Standard HIF model.

coefficient obtained after decomposing with db1 up to level 1. Forth plot of Fig. 5 shows the single value obtained after calculating the standard deviation of approximate coefficients of one cycle current samples. This current feature is the feature that is shown with respect to time in fifth plot of Fig. 5. In fifth plot of Fig. 5, first 20 samples are kept zero because feature will not be produced till it has one cycle samples, thereafter, the standard deviation of each phase current approximate coefficient calculated using the recursive moving window of one cycle is depicted. Sixth plot of Fig. 5 shows the next feature produced i.e. from window 2 (2–21 samples) with respect to time. Seventh plot of Fig. 5 shows the next feature produced i.e. from window 3 (3–22) with respect to time. Similarly, the window will move and produce features with respect to time as shown in last plot of Fig. 5. Feature in this case means the standard deviation feature of the approximate coefficient of three phase current signals obtained after processing with DWT.

Similarly, the feature vectors for each phase currents are obtained. Based on the current feature values for each phase current, different values are obtained for different types of faulty and non-faulty cases. The membership functions were obtained based on rigorous evaluation of different HIF, LIF and various other switching and non-faulty events. With the help of these values, FIS systems are formulated for fault detection and classification.

The reason behind the choice of 'db1' wavelet for wavelet decomposition from the family of Daubechies wavelet, is explained with the help of Fig. 6. Here the feature extraction using db1 and other possible dbx's has been depicted for a HIF case occurred in "*A*" phase at 0.3 s. Fig. 6 (a) shows the phase "*A*" current signals during AG-HIF at 0.3 s. Fig. 6 (b)-(f) shows the features obtained using db1, db2, db4, db8 and db12, respectively. It can be observed from Fig. 6(b) that the features obtained using db1 wavelet show clearly distinct variation after the inception of fault which can be used to distinguish between fault and normal scenario. Whereas the features obtained using other dbx's wavelets are oscillating. Hence, in this work, db1 wavelet has been chosen.

3.3. Design of DWT and FIS based method

The proposed method has two modules i.e. fault detection FIS module and fault classification FIS module. Details description of designing fault detection module and fault classification module has been discussed below.

3.3.1. Design of fault detection FIS module

One of the requirements of fuzzy inference is that it requires expert knowledge of the problem addressed. Hence in this work, current and voltage signals of different fault cases, switching events and normal operation has been studied. After extensive study, different membership functions have been designed for fault detection and classification. After various trial and errors, the final membership function was decided considering the accuracy in detecting fault cases correctly. The fault detection FIS module has been designed using the current features of the three phases using both Sugeno and Mamdani type FIS.

To design the Mamdani type FIS, first the input current feature are fuzzified using membership functions. Based on trial and error with different membership functions, it was concluded that triangular membership function for the Mamdani fuzzy system is suitable. To decide the spreads (ranges) of the membership function triangles, rigorous simulation studies have been performed and input features range, its minimum and maximum value in faulty and healthy phase(s) has been observed such as near end and far end fault with high fault resistance, HIF, different LIF and different normal operating condition such as change in DG parameters, loading condition, and switching events like, capacitor switching, DG switching, load switching, transformer energization etc.

The lower range and upper range of input current features are noted. The whole range is further divided into four different ranges SD1, SD2, SD3 and SD4 depending on the operating scenario. SD1, SD2, SD3 and SD4 are the four input membership functions used in each of the FIS. SD1 is the membership function range for different normal operating conditions which are not faulty. SD2 is the membership function range for different HIF. SD3 is the membership function range for different switching events. SD4 is the membership function range for different LIF.

The degree of membership functions using triangular membership function for phase *A* input current feature is shown in Fig. 5. The output membership function is separated into 'TH' which refers to 'trip high' (output '1') and 'TL' which refers to 'trip low' (output '0'). If the output is '1' the fault is detected and the trip signal will be issued. If the output is '0' then there is no fault is system, so no trip signal is issued. Fuzzification parameters for different FIS designed for phases *A*, phase *B*, phase *C* and ground *G* are shown in Table 1.

The Mamdani based system architecture uses max-min composition method and centroid defuzzification method is used. The rules are based on the behavior of membership function values. For instance, if the input current feature falls in the range of SD1 then the trip signal is TL i.e. 0. The different fuzzy rules were defined as follows:

i If input is SD1 then output is TL.
ii If input is SD2 then output is TH.
iii If input is SD3 then output is TL.
iv If input is SD4 then output is TH.

Similarly, phase *B* and phase *C* FIS were designed following the same

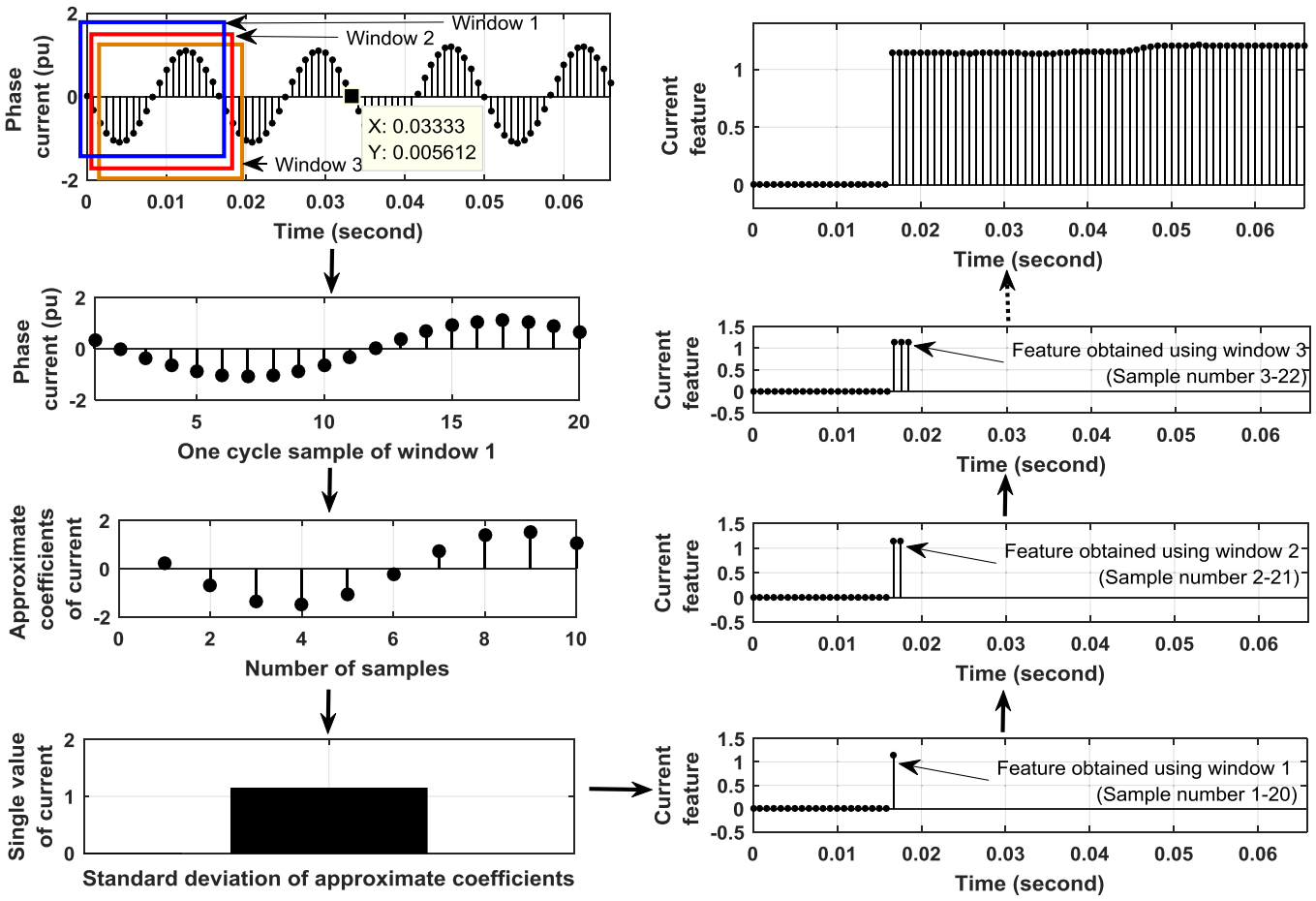

Fig. 5. Signal processing and feature extraction in time domain.

set of rules. The output of all three phase FIS are combined using OR gate to decide whether the system is subjected to fault or not. Finally, the fault detection output is obtained which detects the presence of HIF or LIF or healthy condition.

In the similar fashion, the Sugeno based FIS is designed having rules base and inputs features. Its architecture is built using the Max-Min composition technique with centroid type method used for the process of defuzzification. A type '0' Sugeno system has been used for designing the FIS. A weighted average or weighted sum of some data points is calculated for obtaining the defuzzied output in this case, which makes it computationally more competent in comparison to a Mamdani system which uses a centroid method for this purpose. Fig. 7 shows the adopted membership function for Mamdani type and Sugeno type FIS.

3.3.2. *Design of fault classification FIS module*

Four FIS modules phase *A* FIS, phase *B* FIS, phase *C* FIS and ground *G* FIS for fault classification has been designed. Input to each phase FIS modules are the wavelet processed current features. Input to the ground FIS is the zero sequence current feature. Mamdani FIS for fault classification modules has been designed using the membership functions given in Table 1. Other parameters are kept same as described in the above section for Mamdani FIS. The rules designed for phase *A*, phase *B* and phase *C* are same as for fault detection. The rules designed for ground *G* FIS are as follows:

i If input is ZS1 then output is TL.
ii If input is ZS2 then output is TH.

Similarly, the Sugeno FIS has been designed for phase *A*, phase *B*, phase *C* and ground *G* as described in the above section. The results obtained using Mamdani and Sugeno method has been analysed in the next section.

4. Results and discussion

The proposed DWT and FIS based method is tested with IEEE 13 bus system under various fault scenarios to validate the efficacy. The test system is hybrid in nature and can therefore be considered as a replica of the modern-day distribution systems. Various types of faults such as LIF and HIF have been applied and the analysis is performed on fault data recorded from Bus-650. The addition of DGs in the system effects the fault currents invariably and hence hampers the ability of the protection scheme to detect the faults. Taking into consideration different scenarios such as the effect of change of DG parameters like change in wind speed or irradiance level of the Sun, cases of evolving HIF and LIF faults, faults occurring with varying fault resistances or faults incepted at different inception angles have been simulated and thorough investigation has been performed. These fault cases cover mostly all the commonly occurring situations in the distribution network. The various test studies carried out are discussed in detail in subsequent sub-sections.

4.1. *Performance varying solar DG parameters*

As mentioned previously, modern distribution system is incorporated with various types of DGs. The operating conditions of the DGs keep on changing depending on changes in atmospheric conditions. The two most commonly varying parameters in solar based DGs are irradiance (I) level of the sun and the temperature (T). Keeping in mind the

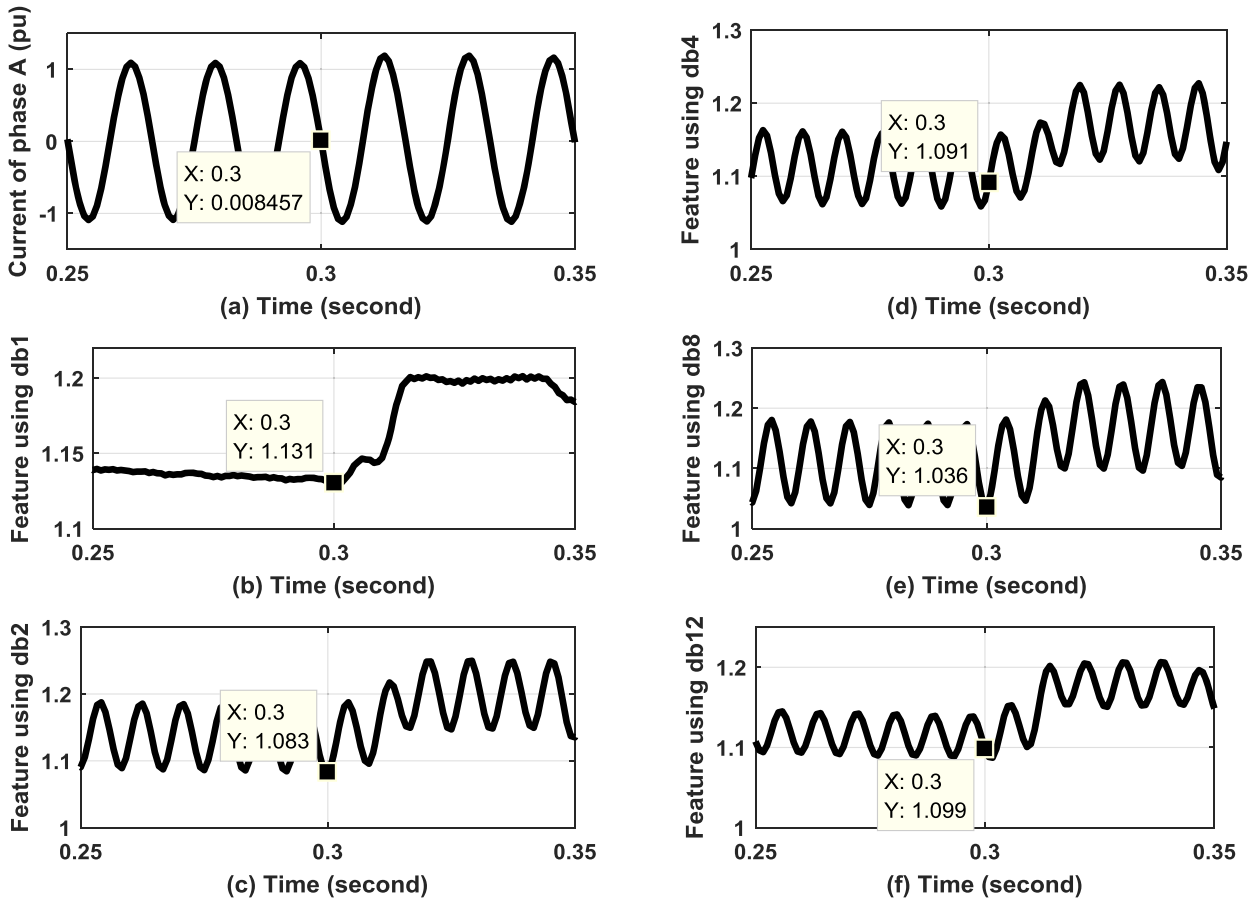

Fig. 6. During AG-HIF at 0.3 s input current and features obtained using various dbx's wavelets (a) Current waveform, (b) db1 wavelet (c) db2 wavelet (d) db4 wavelet (e) db8 wavelet (f) db12 wavelet.

Table 1
Fuzzification parameters for different FIS using membership function.

Membership function Type	FIS	Membership function name	Membership function range Low	Medium	High
Input	Phase *A*	SD1	0.0000	0.5810	1.1630
		SD2	1.1630	1.1690	1.1850
		SD3	1.1850	1.2770	1.3700
		SD4	1.3700	1.6350	1.9000
	Phase *B*	SD1	0.0000	0.5750	1.1501
		SD2	1.1501	1.1717	1.1934
		SD3	1.1934	1.2817	1.3700
		SD4	1.3700	1.6350	1.9000
	Phase *C*	SD1	0.0000	0.5599	1.1198
		SD2	1.1198	1.1388	1.1578
		SD3	1.1578	1.2639	1.3700
		SD4	1.3700	1.6350	1.9000
	Ground *G*	ZS1	0.0000	0.0154	0.0376
		ZS2	0.0376	0.0645	1.0000
Output	Fault Detection Output	TL	-0.5000	0.0000	0.5000
		TH	0.5000	1.0000	1.5000

changes in these parameters, various case studies have been performed for both HIF and LIF type of fault. The Rp and Rn values vary from 40 to 150 Ω in HIF and the resistance is 0 Ω in LIF for all fault cases. The results are tabulated in Table 2 for both Mamdani and Sugeno type FIS systems. The irradiance level has been varied from $I = 800$ to 1000 W/m^2 to 1000 W/m^2. Similarly, temperature variation between 40°C and 50°C has been taken into consideration. It can be observed that, fault detection time required by both the fuzzy systems is nearly same. The response of fault detection and fault classification schemes for AG type HIF created at 0.3 s with irradiance $I = 800$ W/m^2 and temp 40 °C are depicted in Fig. 8 and Fig. 9, respectively. Fig. 8 (a) and (b) shows the three phase current and variation of the input feature of phase *A*, respectively. Fig. 8 (c) and (d) shows the fault detection output obtained by Mamdani FIS and Sugeno FIS, respectively. Fig. 9 shows the fault classification output of Mamdani FIS for phase *A*, phase *B*, phase *C* and ground. Fig. 9 (a-d) shows the output of phase *A, B, C* and ground *G*, respectively. As different FIS has been designed for the three phases and ground detection, therefore the fault detection time will be different in the output of phase and ground. The overall trip signal of the proposed technique will be given according to the fault detection output as shown in Fig. 2. As all three phases are connected through "OR" gate for fault detection thus as soon as any one output goes high, the trip signal is issued to circuit breaker. It is evident that the proposed scheme clearly detects the presence of fault and classifies the faulty phase correctly. Thus, the proposed method is not affected by change in solar DG parameter during HIF and LIF.

4.2. Performance during varying wind DG parameters

The proposed method is tested with changes in wind DG parameter for both HIF and LIF faults. The Rp and Rn values vary from 40 to 150 Ω in HIF and the resistance is 0 Ω in LIF for all fault cases. The wind speed has been varied between ώ = 14 and ώ = 18 m/s. One of the test case is shown in Fig. 10 for fault detection during ABG fault at 0.3 s with wind speed ώ = 15 m/s. Fig. 10 (a) and (b) shows the three phase current and variation of the input feature of, respectively. Fig. 10 (c) and (d) shows the fault detection output obtained by Mamdani FIS and Sugeno FIS, respectively. The test results of Mamdani and Sugeno FIS systems in detecting the faults varying wind speed are shown in Table 3. The fault

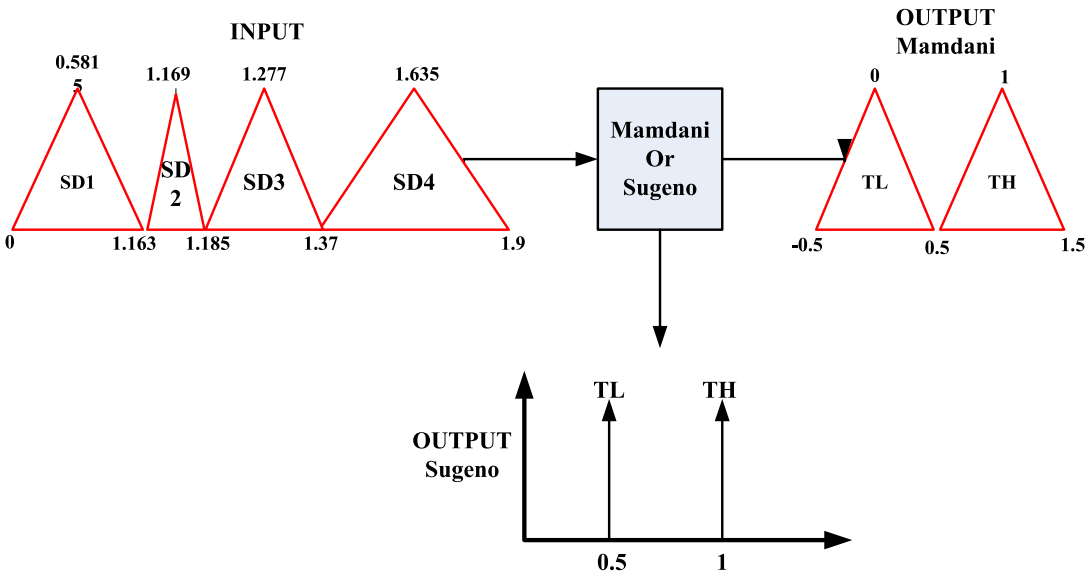

Fig. 7. Adopted membership function for Mamdani and Sugeno type FIS.

Table 2
Performance of the proposed method varying solar DG parameters.

Fault	DG parameter	Fault Type	Time required for detection of fault by FIS (seconds)	
			Mamdani	Sugeno
HIF	I = 800, T = 40 °C	AG	0.0042	0.0042
	I = 800, T = 45 °C	ABG	0.0017	0.0017
	I = 800, T = 50 °C	ABCG	0.0017	0.0017
	I = 900, T = 40 °C	BG	0.0025	0.0025
	I = 900, T = 45 °C	BCG	0.0025	0.0025
	I = 900, T = 50 °C	ABCG	0.0025	0.0025
	I = 1000, T = 40 °C	CG	0.0075	0.0075
	I = 1000, T = 45 °C	CAG	0.0075	0.0075
	I = 1000, T = 50 °C	ABCG	0.0025	0.0025
LIF	I = 800, T = 40 °C	AG	0.0017	0.0017
	I = 800, T = 45 °C	ABG	0.0025	0.0025
	I = 800, T = 50 °C	ABCG	0.0017	0.0017
	I = 900, T = 40 °C	BG	0.0034	0.0034
	I = 900, T = 45 °C	BCG	0.0042	0.0042
	I = 900, T = 50 °C	ABCG	0.0017	0.0017
	I = 1000, T = 40 °C	CG	0.0025	0.0025
	I = 1000, T = 45 °C	CAG	0.0025	0.0025
	I = 1000, T = 50 °C	ABCG	0.0017	0.0017

detection time as observed from Table 4 in case of HIFs is more in comparison with LIFs. Results shows that proposed method is not affected change in wind speed.

4.3. Performance during varying both wind and solar DGs parameters

The IEEE -13 bus systems is incorporated with various DGs such as solar or wind-based DG etc. Wind and solar DG particularly are highly dependent on the ever changing weather conditions. For instance, there can be a change in the irradiance level of the Sun, change in temperature or a change in wind speed. Keeping in mind the changing atmospheric conditions, studies have been conducted by varying these parameters. Three parameters have been varied namely wind speed (ώ (m/s)), solar irradiance $(I(W/m^2))$ and temperature (T). The wind speed is varied between 13 and 18 m/s, solar irradiance between 800 and 1000 W/m^2 and temperature between 40 and 50 °C. The effect of all of these parameter variations have been studied for various types of HIF faults. The Rp and Rn values vary from 40 to 150 Ω in HIF and the resistance is 0 Ω in LIF for all fault cases. The test results for the same are tabulated in Table 4 for both Mamdani and Sugeno FIS. From the results obtained it can be observed that fault detection time is between quarter to four cycles in case of simultaneously varying both wind and solar DGs parameters. Hence the proposed scheme is efficient in detecting the HIF with DG parameter change.

4.4. Performance during varying fault inception angle

Fault in a system can occur at any point of time and the fault detection method should be able to detect the fault. To investigate the effect of fault inception angle on the distribution system, various HIF and LIF faults have been simulated. The Rp and Rn values vary from 40 to 150 Ω in HIF and the resistance is 0 Ω in LIF for all fault cases. The inception angle has been varied between 0^0 and 360^0. Fig. 11 shows one test fault cases for Sugeno FIS during AB-LIF at 0.3 s in 45 ° fault inception angle. Fig. 11 (a) and (b) shows the three phase current and variation of the input feature of, respectively. Fig. 11 (c)–(f) shows the fault classification output obtained Sugeno FIS. Table 5 gives an insight into how with the change in fault inception angle, the time to detect the fault varies. Here for solar DG solar irradiance is kept as $I = 1000\ W/m^2$ and for wind DG the wind speed is taken as ώ = 15 m/s. But nonetheless both the FIS systems are able to detect the fault in all the cases efficiently. Results show that the proposed method is not affected by change in fault inception angle.

4.5. Performance during varying fault resistance for LIF

Although the work focuses on detection and classification of HIF in distribution system, LIF are also tested. The LIF are those faults which involve fault resistance values between 0 and 20Ω, thereby the magnitude of the fault current is more as compared to HIF. Different types of low impedance faults have been simulated and the results of some of the case studies is tabulated in Table 6. The time taken for detection of LIF is very less as it can be observed from the results depicted in Table 5. The proposed DWT and FIS based method is not affected by LIF.

4.6. Performance during evolving faults

To validate the usefulness of the proposed scheme, case study on evolving faults is also performed. An evolving fault is one in which multiple types of faults occur one after another in short period of time. For instances, an evolving fault can initially be a single line to ground fault which may convert into a double line to ground fault or initially a

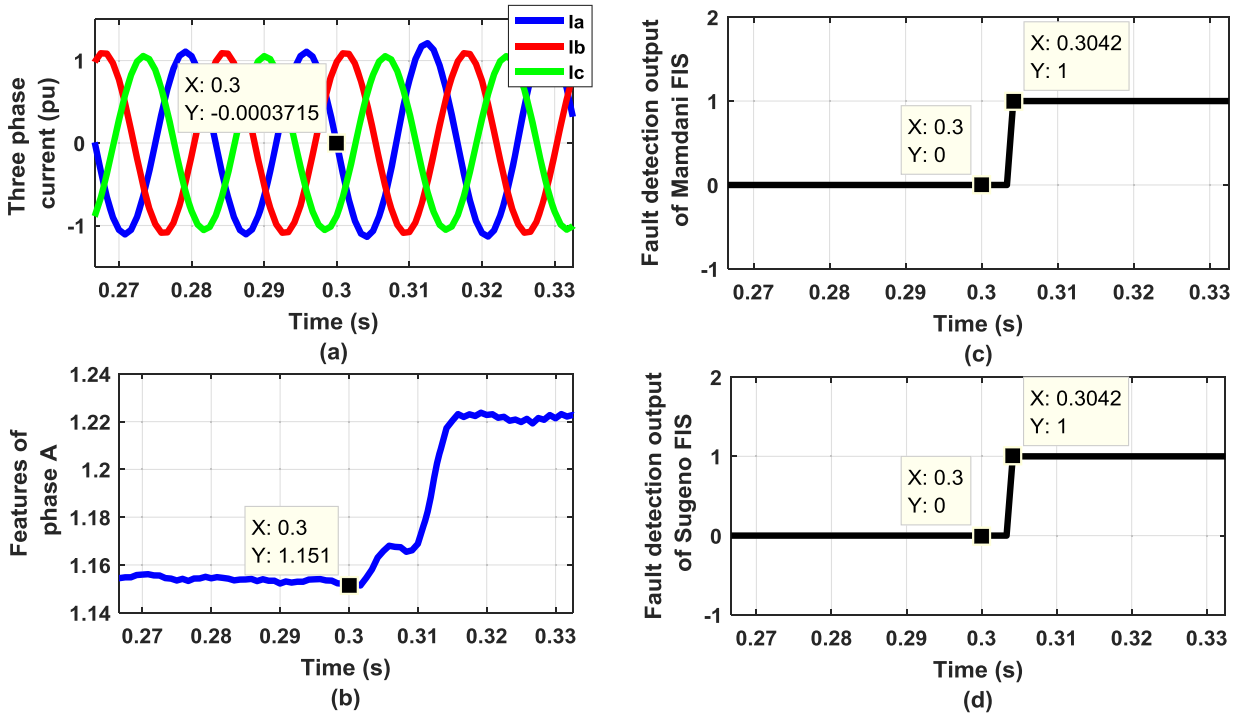

Fig. 8. Fault detection during AG fault at 0.3 s with irradiance $I = 800\ W/m^2$ and $T = 40\ °C$ (a) Three phase current signals (b) Features obtained from phase A current (c) Output of fault detection for Mamdani FIS (d) Output of fault detection for Sugeno FIS.

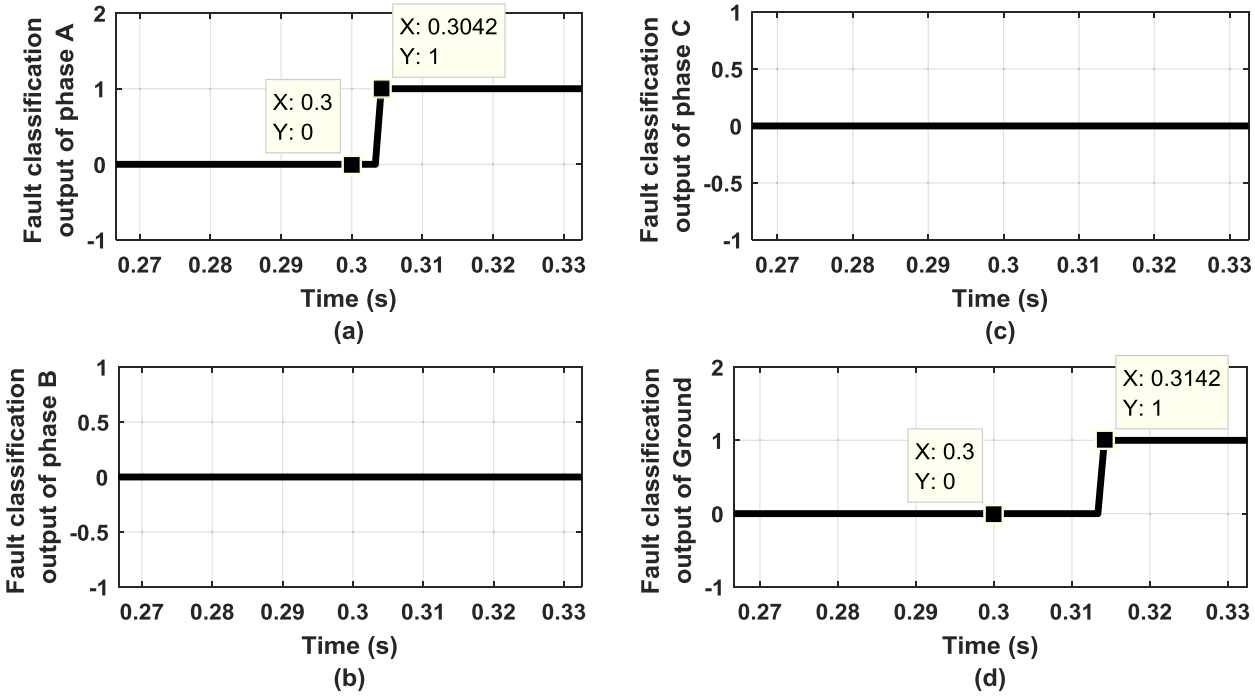

Fig. 9. Fault classification during AG fault at 0.3 s with irradiance $I = 800\ W/m^2$ and $T = 40\ °C$ for Mamdani FIS (a) Output of fault classification for phase A (b) Output of fault classification for phase B (c) Output of fault classification for phase C (d) Output of fault classification for ground G.

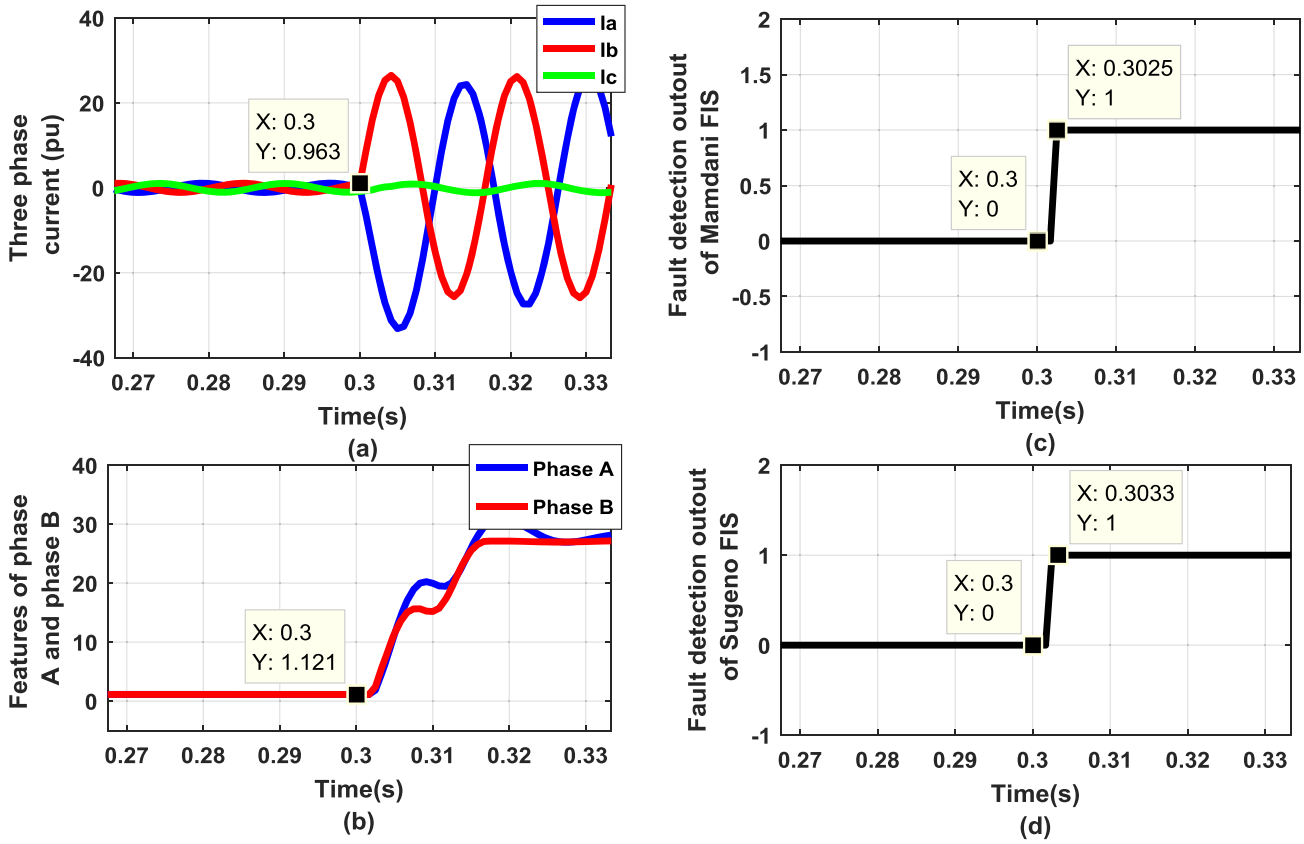

Fig. 10. Fault detection during ABG-LIF fault at 0.3 s with wind speed ώ = 15 m/s (a) Three phase current signals (b) Features obtained from phase *A* to phase *B* current (c) Output of fault detection for Mamdani FIS (d) Output of fault detection for Sugeno FIS.

Table 3
Performance of the proposed method varying wind DG parameters.

Fault	Wind speed (m/s)	Fault Type	Time required for detection of fault by FIS (seconds)	
			Mamdani	Sugeno
HIF	ώ = 14	AG	0.0650	0.0650
	ώ = 15	ABG	0.0083	0.0083
	ώ = 16	ABCG	0.0092	0.0092
	ώ = 17	BG	0.0100	0.0100
	ώ = 18	BCG	0.0142	0.0142
LIF	ώ = 14	AG	0.0017	0.0017
	ώ = 15	ABG	0.0017	0.0017
	ώ = 16	ABCG	0.0058	0.0058
	ώ = 17	BG	0.0017	0.0017
	ώ = 18	BCG	0.0067	0.0067

Table 4
Performance during varying solar DG and wind DG parameters.

Fault	DG parameter	Fault Type	Time required for detection of fault by FIS (in sec.)	
			Mamdani	Sugeno
HIF	ώ = 13,I = 800, T = 45°	AG	0.0783	0.0783
	ώ = 14, I = 800, T = 45°	ABG	0.0625	0.0625
	ώ = 14, I = 800, T = 40°	ABCG	0.0625	0.0625
	ώ = 15, I = 900, T = 45°	CG	0.0092	0.0092
	ώ = 16, I = 900, T = 50°	BCG	0.0383	0.0383
	ώ = 16, I = 900, T = 45°	ABCG	0.0375	0.0375
	ώ = 17, I = 1000, T = 45°	ACG	0.0300	0.0300
	ώ = 18, I = 1000, T = 45°	BG	0.0183	0.0183
LIF	ώ = 13,I = 800, T = 45°	AG	0.0017	0.0017
	ώ = 14, I = 800, T = 45°	ABG	0.0033	0.0033
	ώ = 14, I = 800, T = 40°	AB	0.0058	0.0058
	ώ = 15, I = 900, T = 45°	ABCG	0.0050	0.0050
	ώ = 16, I = 900, T = 50°	BG	0.0033	0.0033
	ώ = 16, I = 900, T = 45°	BCG	0.0017	0.0017
	ώ = 17, I = 1000, T = 45°	BC	0.0025	0.0025
	ώ = 18, I = 1000, T = 45°	ABC	0.0017	0.0017

double-line-ground fault occurs which may further convert into a triple-line-ground fault. The Rp and Rn values vary from 40 to 150 Ω in HIF and the resistance is 0 Ω in LIF for all fault cases. Some of the test results corresponding to such cases have been evaluated and the results are presented in Table 7.

Fig. 12 represents one such case graphically where BG type of fault has occurred at 0.3 s which later gets converted into a BCG type fault at 0.3033 s. Fig. 12 (a) shows the three phase current signals and Fig. 12 (b) shows the features obtained from phase *B* to phase *C* current. Fig. 12 (c) shows the output of fault detection for Mamdani FIS and Fig. 12 (d) shows the three output of fault detection for Sugeno FIS. The proposed method detects the evolving faults correctly for all the tested fault cases.

4.7. *Performance with noisy signals*

The current and voltage signals in the system can invariably get altered by presence of noise in the system. To test the scheme ability in any such unforeseen circumstances, fault current signals are intentionally added with white Gaussian noise with a signal to noise ratio (SNR) varying between 30 and 50 dB. Lower the SNR more is the noise content. The Rp and Rn values vary from 40 to 150 Ω in HIF and the resistance is

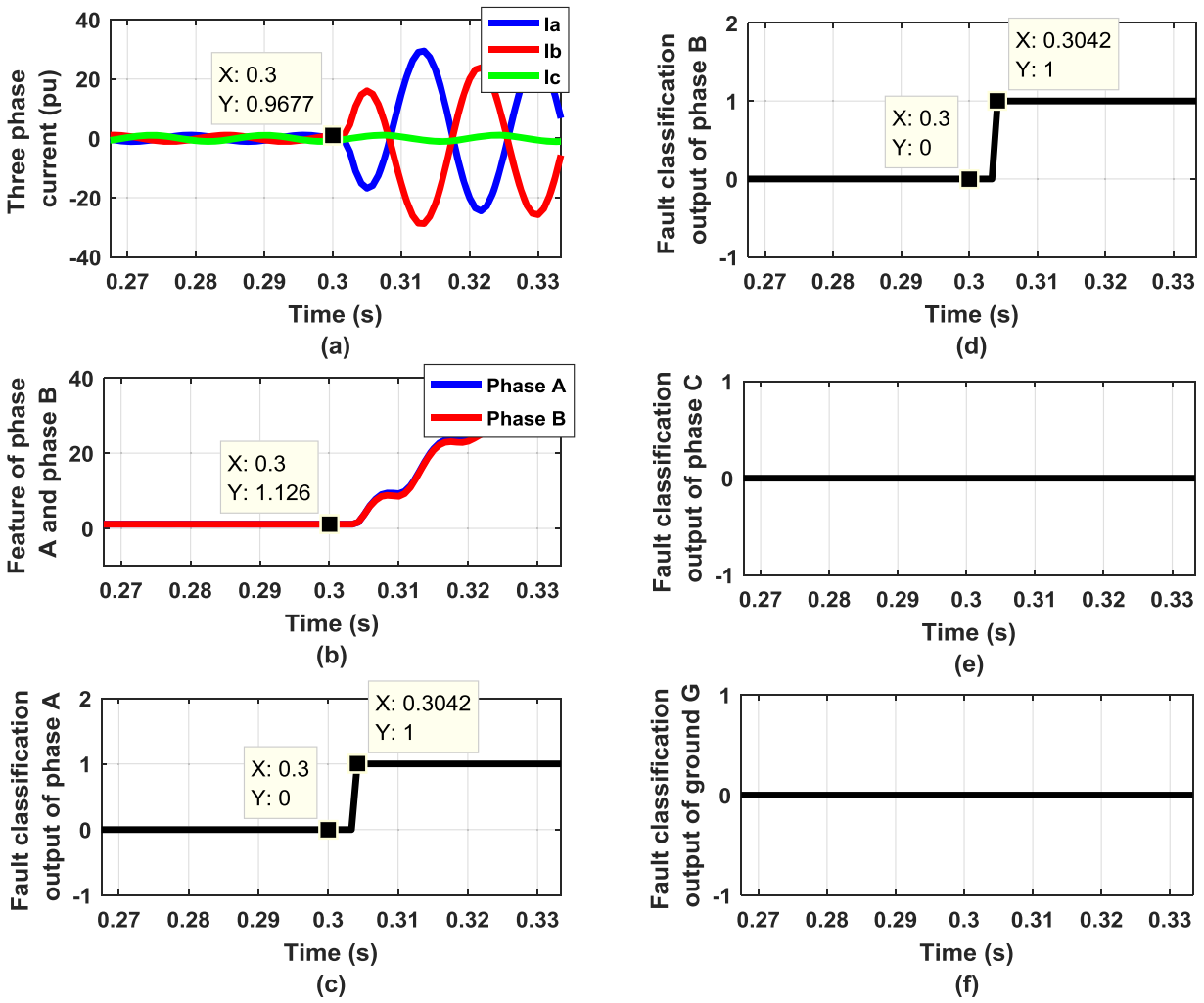

Fig. 11. Fault classification for Sugeno FIS during AB-LIF fault at 0.3 s in 45^0 fault inception angle (a) Three phase current signals (b) Features obtained from phase *A* to phase *B* current (c) Output of fault classification of phase *A* (d) Output of fault classification of phase *B* (c) Output of fault classification of phase *C* (f) Output of fault classification of ground *G*.

Table 5
Performance during varying fault inception angle.

Fault	Fault inception angle (0)	Fault Type	Time required for detection of fault by FIS (seconds) Mamdani	Sugeno
HIF	0	BG	0.0575	0.0575
	45	AG	0.0725	0.0725
	90	ABCG	0.0125	0.0125
	135	BCG	0.0650	0.0650
	180	CG	0.0575	0.0575
	300	ABG	0.0250	0.0250
	360	AG	0.0283	0.0283
LIF	0	AG	0.0017	0.0017
	45	AB	0.0033	0.0033
	90	ABG	0.0058	0.0058
	135	ABC	0.0075	0.0075
	180	ABCG	0.0092	0.0092
	300	BG	0.0158	0.0158
	360	BCG	0.0183	0.0183

Table 6
Performance during varying fault resistance.

Fault	Fault Resistance (Ω)	Fault Type	Time required for detection of fault by FIS (seconds) Mamdani	Sugeno
LIF	0	AB	0.0017	0.0017
	2	ACG	0.0058	0.0058
	4	BCG	0.0025	0.0025
	6	ABG	0.0033	0.0033
	8	ABCG	0.0167	0.0167
	10	AG	0.0108	0.0108
	13	BG	0.0092	0.0092
	16	CG	0.0167	0.0167
	20	ABCG	0.0033	0.0033

0 Ω in LIF for all fault cases. Fig. 13. shows the performance during CG-HIF occurring at 0.3 s. Fig. 13 (a) shows the phase *C* current signals with 30 dB noise and without noise. Fig. 13 (b) shows the features obtained from phase *C* current with 30 dB noise and without noise. Fig. 13 (c) shows the output of fault detection module for Mamdani FIS for signals with 30 dB noise. Fig. 13 (d) shows the output of fault detection for Sugeno FIS for signals with 30 dB noise. From Fig. 13 it can be observed that proposed method can detect faults correctly for noisy signals. Table 8 shows analysis for varying HIF and LIF faults with different levels of noise added in the signals. It can be seen that even with presence of noise in the signals, the fuzzy system has been able to identify the fault rapidly and accurately.

Table 7
Response time of FIS for detecting evolving faults.

Fault	Fault type I	Fault type II	Fault inception time1 (s)	Fault inception time2 (s)	Time required for detection of fault by FIS (seconds)	
					Mamdani	Sugeno
HIF	ABG	ABCG	0.3	0.3021	0.0033	0.0033
	AG	ABG	0.3	0.3021	0.005	0.005
	BG	BCG	0.3	0.3021	0.0033	0.0033
	ABCG	CG	0.3	0.3021	0.0017	0.0017
	AG	BG	0.3	0.3021	0.0242	0.0242
LIF	AG	ABCG	0.3	0.3021	0.0023	0.0023
	ABG	BG	0.3	0.3021	0.0010	0.0010
	CG	ACG	0.3	0.3021	0.0021	0.0021
	ABCG	CG	0.3	0.3021	0.0007	0.0007
	BCG	BG	0.3	0.3021	0.0410	0.0410

4.8. Performance during switching events and non-fault conditions

4.8.1. Induction motor load switching

Sometimes some non-faulty events occur in the system which if not identified accurately can lead to false tripping of the relay. A 36 kW induction motor load connected near bus 632 is switched into the system at 0.3 s. This motor acts as sudden load for the system and is also a non faulty event. The results in this case as shown in Fig. 14 demonstrate that the fuzzy systems do not issue a trip command and successful in identifying this case as non-faulty event. Sometimes in case of distribution systems, the load keeps on varying depending on the demand. Therefore to test this case the motor load is switched in and switched out from the system in 0.05 s.

4.8.2. Capacitor switching

Another non-faulty event that may occur in the system is capacitor switching event. Three phase capacitor bank with rating of 250 KVAr is connected near bus 650 and switched into the system at 0.3 s. It has been observed that the output of the fault detector remain low at all times treating this event as no fault. In another case another capacitor bank of 300 KVAr is switched into the system. The proposed method detects this condition also as no fault.

4.8.3. Impact of DG switching

The addition of DG in the distribution network leads to a change in the fault current level often confusing the traditional protection schemes. Due to varying levels of fault current in the downstream, the relay present in the upstream at the substation gets blinded and leads to false or delayed tripping of the relay. Also the DGs can be switched in and out depending on the load requirements which lead to transients. The solar and wind DGs are switched in and out of the system and its effect has been studied on the system to check the robustness of the proposed scheme. Fig. 15 shows the output of fault detection in case of solar DG switching. Fault detection output proves that there is no fault in the system. The proposed method is robust against the switching events and treats it as non-faulty case.

4.8.4. Impact of transformer energization

Switching in and out of a transformer leads to high inrush current flow which can be visualized as an over current accompanied with sag in voltage. This effect is caused by saturation of the magnetic circuit. The overcurrent transients last up to a few cycles in comparison with HIFs whose transients can last up to a few minutes to hours. It is observed that these transients last for only a few cycles and the algorithm is also triumphant in determining this as a non-faulty event.

4.8.5. Impact of non-linear load switching

Proposed method is also tested with non-linear and harmonic load switching (LSW). A single phase non-linear load is switched into the system. A single phase bridge rectifier in conjugation with a capacitor filter is used to replicate the non-linear load model and such models are attached to each phase. It causes a harmonic disturbance in the current and voltage signals. It has been observed that the current signals show

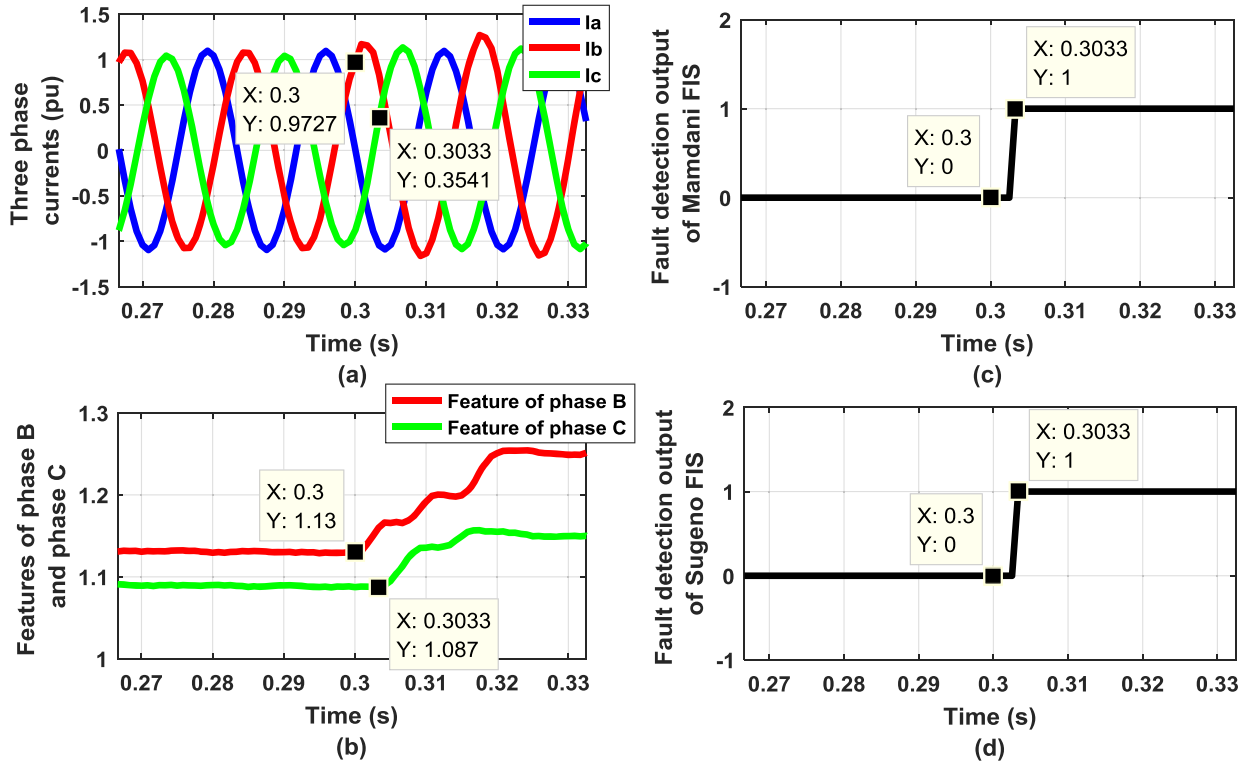

Fig. 12. Performance during BG type of fault is occurring at 0.3 s which later gets converted into a BCG type fault at 0.3033 s (a) Three phase current signals (b) Features obtained from phase *B* to phase *C* current (c) Output of fault detection for Mamdani FIS (d) Output of fault detection for Sugeno FIS.

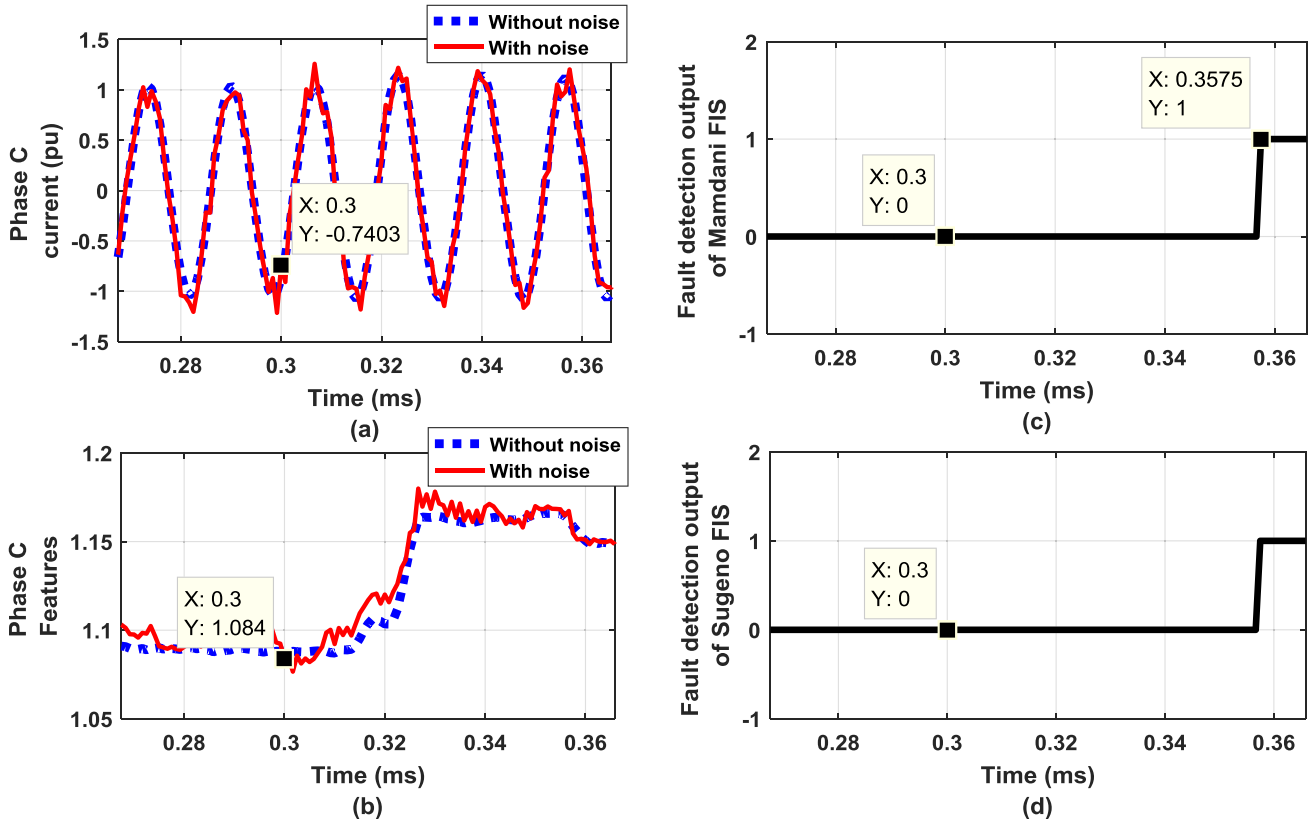

Fig. 13. Performance during CG-HIF occurring at 0.3 s (a) *Phase C* current signals with 30 dB noise and without noise (b) Features obtained from phase *C* current with 30 dB noise and without noise (c) Output of fault detection for Mamdani FIS for signals with 30 dB noise (d) Output of fault detection for Sugeno FIS for signals with 30 dB noise.

Table 8
Performance of the method with noisy signals.

Fault	SNR (dB)	Fault Type	Time required for detection of fault by FIS (seconds)	
			Mamdani	Sugeno
HIF	30	AG	0.0283	0.0283
	30	ACG	0.0308	0.0308
	40	CG	0.0117	0.0117
	40	BCG	0.0133	0.0133
LIF	30	AG	0.0108	0.0108
	30	BG	0.0025	0.0025
	40	CG	0.0017	0.0017
	40	ABCG	0.0017	0.0017

some distortion. In this case the output of the proposed scheme is low throughout, thus treating the event as non-faulty. To make the study even more extensive analysis has been done by switching in just one phase of the load as in most of the distribution systems the load at times is of single phase in nature. In this case also the FIS is able to identify the event as non-faulty.

4.8.6. Performance in case of IEEE 33-bus distribution test system

To validate the proposed scheme for bigger test system, an IEEE 33-bus distribution test system has been utilized as shown in Fig. 16. It is a radial distribution system consisting of thirty-three buses and thirty -two branches. The voltage level of each bus is 12.66 kV. A synchronous generator feeds the system and is loaded from 2.3 MVar to 3.715 MW loads connected to all the branches having a different power factor. The length of each branch is 1 km. The operating frequency of the system is 50 Hz and sampling frequency is 1 kHz.

HIF and LIF test cases have been simulated on this system and the results are tabulated in Table 9. It can be observed that db1 wavelet for feature extraction and FIS for fault detection and classification are efficient in detecting faults for this bigger system as well. The output for fault detection for an AG type HIF fault incepted at 0.3 s has been shown in Fig. 17. Time taken for detecting both HIF and LIF is less than 0.25 cycle. Hence the proposed scheme is efficient in detecting faults in more complex and bigger distribution systems as well.

5. Comparative assessments

The performance of the fault detection and classification module has been analysed using the number of fault cases used for testing the proposed method and the number of fault cases accurately detected as fault or no fault. A total of 22,500 cases are considered varying different operating conditions as mentioned in result section. All the tested cases have detected and classified the faults and non-fault situations correctly. The time required for feature extraction using DWT is nearly 0.06 s i.e., nearly 4 cycles in 11th Gen Intel(R) Core(TM), i5-1135G7@2.40 GHz, 16 GB RAM computer. Therefore, in case of HIF, the whole process, starting from obtaining signals to issue of trip signal takes overall detection time of minimum 4.4 cycles i.e., 0.00425 s to a maximum of 8 cycles i.e., 0.133 s time. On the other hand, in case of LIF, the overall detection time offered by proposed scheme is minimum 4.4 cycles to a maximum of 6 cycles detection time. Hence, it can be said that the proposed DWT and FIS based method is 100% accurate for both LIF and HIFs. A comparative analysis with other presently reported schemes is shown in Table 10.

There are many papers involving use of wavelet transform and soft computing techniques such as ANN, SVM, DT for classification/decision criteria but there are very few papers reported in literature which uses fuzzy inference system [8,19] along with wavelet transform [19] for

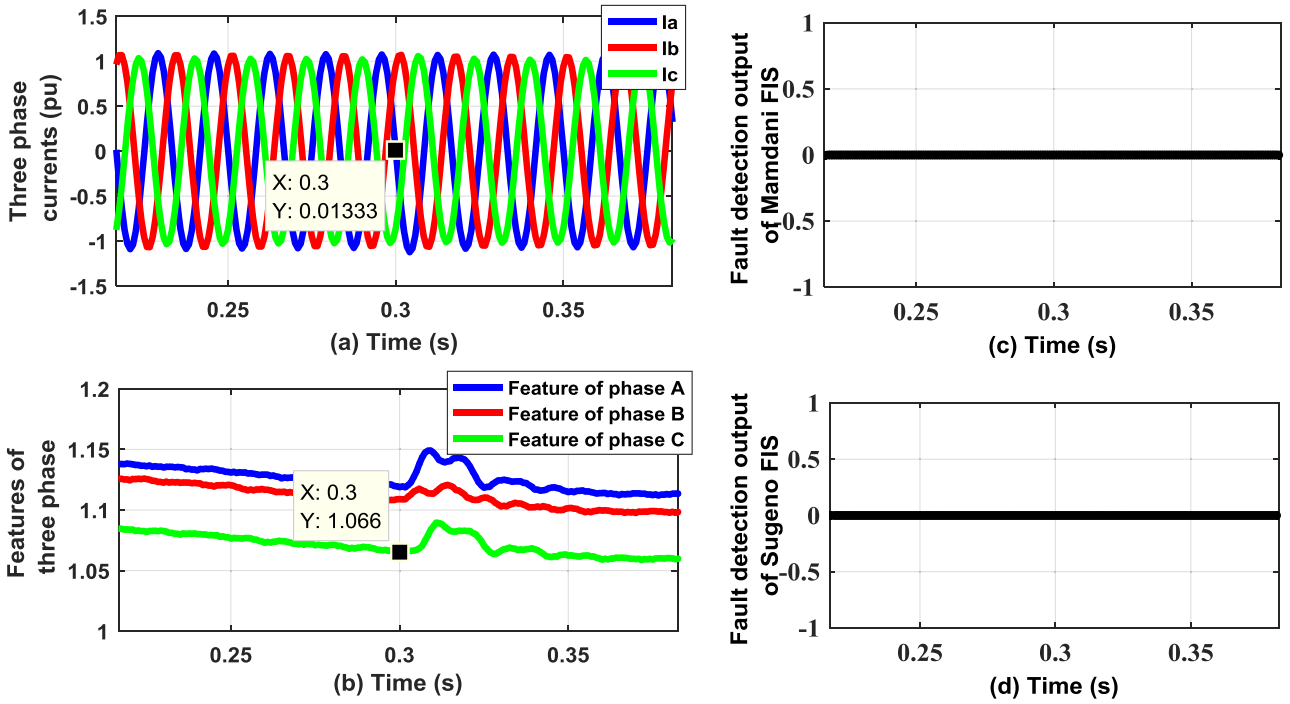

Fig. 14. Performance during motor load switching (a) Three phase current signals (b) Features obtained from three phase currents (c) Output of fault detection for Mamdani FIS (d) Output of fault detection for Sugeno FIS.

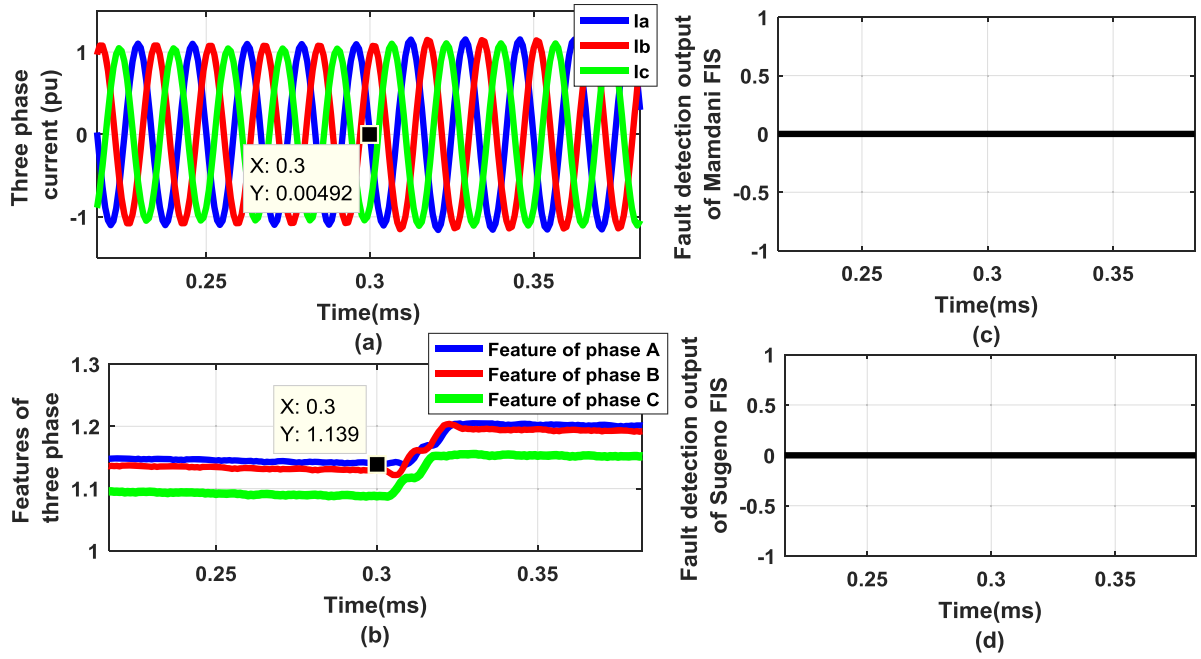

Fig. 15. Performance during solar DG switching (a) Three phase current signals (b) Features obtained from three phase currents (c) Output of fault detection for Mamdani FIS (d) Output of fault detection for Sugeno FIS.

HIF. But these papers have not considered the impact of EVF, non-linear load switching and DGs integration etc. The proposed scheme is suitable for detection of both HIF and LIF. The proposed scheme based on DWT and Fuzzy inference system has been tested for IEEE 13 Bus system and IEEE 33 bus system, it considers the effects of various DGs, switching events and impact of noise etc. Additionally in traditional overcurrent relays, the inverse time characteristics are employed, so based on the magnitude of the current, the time of operation of the relay is calculated. If the magnitude of current is high then time of operation will be less, and vice versa. As per IEC/IEEE, the operating time of extremely inverse solid-state OCR with TMS = 1 and PSM = 2 for LIF is minimum 100 ms to maximum 2 s. In case of HIF, IED/OCR fails to operate, whereas the proposed scheme offers minimum 4.4 cycles i.e., 4.25 ms to a maximum of 6 cycles i.e., 100 ms time detection time for LIF and minimum 4.4

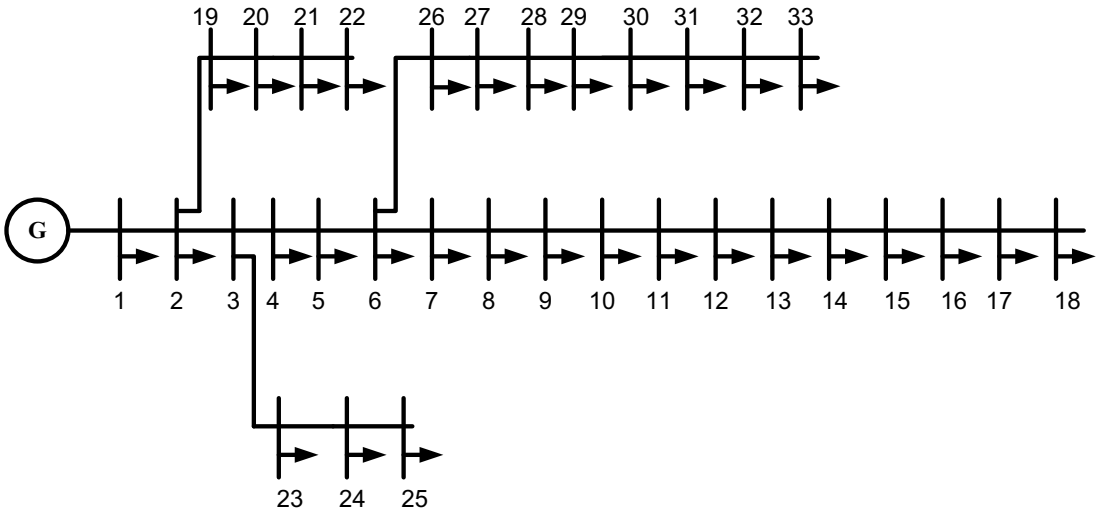

Fig. 16. Single line diagram of IEEE-33 bus system.

Table 9
FIS response time HIF and LIF detection for IEEE 33-bus system.

Type	Fault	FIS Response Time (s)			
		Phase A	Phase *B*	Phase *C*	Ground *G*
HIF	AG	0.0050	-	-	0.0020
	BG	-	0.0030	-	0.0020
	BCG	-	0.0030	0.0035	0.0020
	ABCG	0.0050	0.0030	0.0035	0.0020
LIF	CG	-	-	0.0030	0.0020
	AB	0.0030	0.0020	-	-
	ABG	0.0030	0.0020	-	0.0020
	ABCG	0.0030	0.0020	0.0030	0.0020

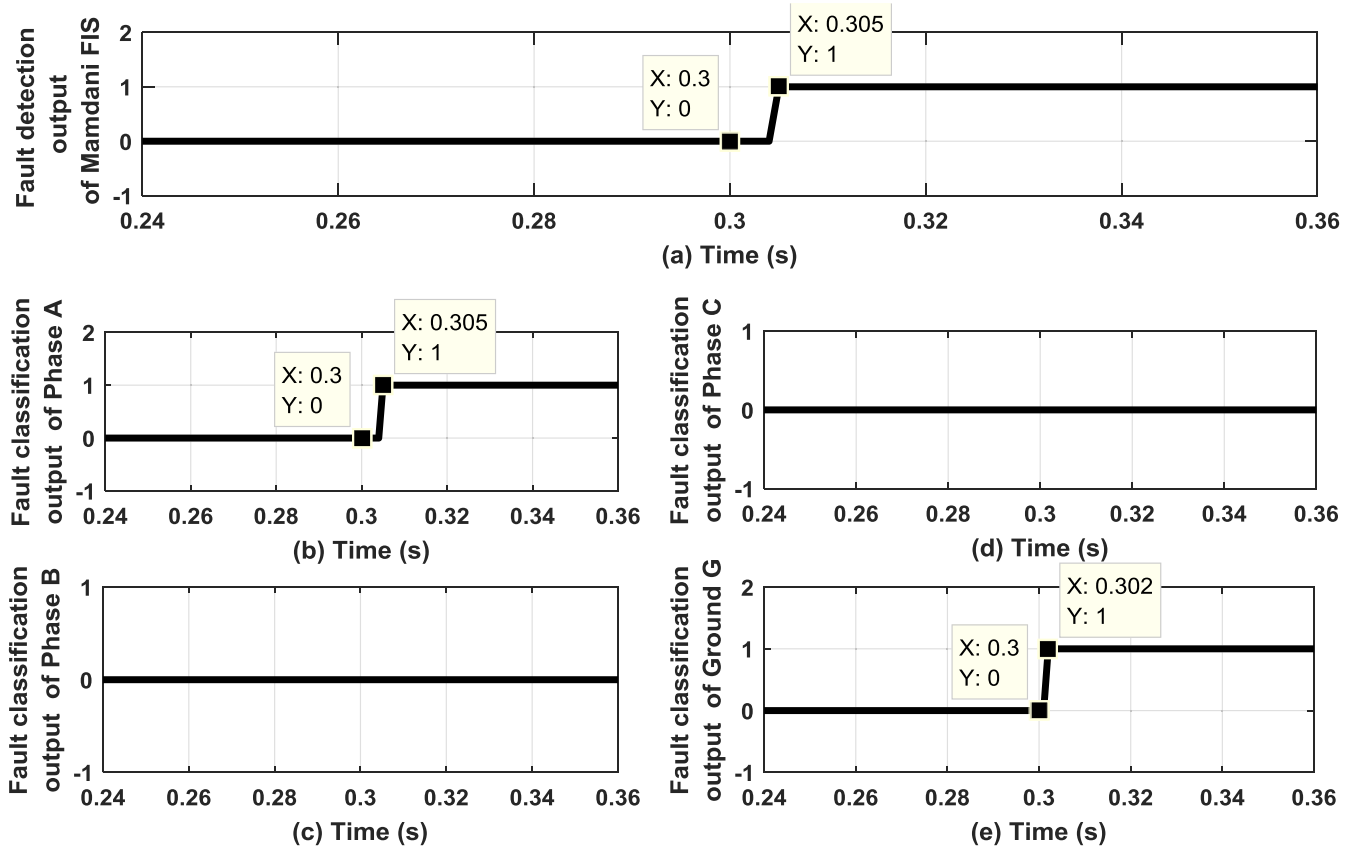

Fig. 17. Output for fault detection and classification using Mamdani FIS for AG –HIF incepted at 0.3 s in IEEE 33-bus system (a) Fault detection output (b) Fault classification output of phase *A* (c) Fault classification output of phase *B* (d) Fault classification output of phase *C* (e) Fault classification output of ground.

Table 10
Comparative analysis with different schemes.

Classification Method	Domain of analysis	Measurement Signal	Accuracy	Test of SE	Test of addition of noise	Test of addition of DG in the system
Neural Network and wavelet [17]	Time-frequency	Current	99.9%	Yes	No	No
Joint time-frequency moment and SVM [18]	Time-frequency	Current	93.6%	Yes	No	No
SVM and VMD [20]	Time-frequency	Current	98.8%	Yes	Yes	Yes
TEKO and VMD [12]	Time-frequency	Current and voltage	NA	Yes	No	No
Morphological Gradient with Fuzzy Logic [28]	Time	Current	99.3%	Yes	No	No
Computational algorithm [29]	Frequency	Current	NA	No	No	No
Proposed Scheme	Time-frequency	Current	100%	Yes	Yes	Yes

cycles (4.25 ms) to maximum 8 cycles i.e., 133 ms detection time for HIF, which is significant advantage over existing relays.

6. Conclusions

In this paper combined DWT and Fuzzy inference system has been utilized for fault detection and classification in distribution system integrated with DGs. DWT has been used for determining the features of the faulty and non-faulty signals and a fuzzy inference system is then developed to detect the fault and classify these signals. All the three phases and ground have their individual FIS to detect and classify the faults. The proposed scheme is suitable for detection of both HIF and LIF. The proposed scheme based on DWT and Fuzzy inference system has been tested for IEEE 13 Bus system and IEEE 33 bus system. It considers the effects of various DGs, switching events and impact of noise. The scheme has been able to distinguish between different conditions such as transformer energization, capacitor bank switching, load switching, evolving faults. The proposed method detects all the tested cases correctly with 100% accuracy, hence it is reliable. In case of HIF, IED/OCR fails to operate, whereas the proposed scheme offers 4.4 cycles to 6 cycles detection time for LIFs and minimum 4.4 cycles to maximum 8 cycles detection time for HIF, which is significant advantage over existing relays. After rigorous analysis obtained from several simulation studies and comparative investigation, it can be concluded that the technique showcases an anticipated performance and can prove to be a good solution in this regard. The future scope of current study lies in the extension of the proposed scheme for detection of fault during islanding condition. Furthermore, the fuzzy based scheme can be designed and examined for fault location estimation task which is helpful to the repair crew for faster supply restoration.

CRediT authorship contribution statement

Maanvi Bhatnagar: Data curation, Investigation, Methodology, Software, Validation, Writing – original draft. **Anamika Yadav:** Conceptualization, Supervision, Writing – review & editing. **Aleena Swetapadma:** Conceptualization, Supervision, Formal analysis, Investigation, Writing – review & editing.

Declaration of Competing Interest

The authors declare that they have no known competing financial interests or personal relationships that could have appeared to influence the work reported in this paper.

Appendix A

Modifications made to the IEEE 13 bus test system.

DG Source	Components	Sub-components
Battery Energy storage system (BESS) -200 kWH capacity	Battery and bidirectional DC-AC inverter.	2-level Voltage source converter (VSC), 120V DC Voltage Source
Solar power plant -Capacity 0.3 MW	Photo voltaic (PV) panel and inverter.	4 PV arrays, DC-DC Converter and VSC.
Wind power plant- Capacity 1.5 MW	Wind turbine generator	Doubly-fed induction generator (DFIG).
Diesel Generator -Capacity 3.125 MVA	Synchronous diesel generator	-

References

[1] S. Kumari, S. De, P.K. Nayak, High impedance fault detection in electrical power distribution systems using moving sum approach, IET Sci. Meas. Technol. 12 (2018) 1–8, https://doi.org/10.1049/iet.-smt.2017.0231.

[2] A. Soheili, J. Sadeh, R. Bakhshi, Modified FFT based high impedance fault detection technique considering distribution non-linear loads: simulation and experimental data analysis, Int. J. Electr. Power Energy Syst. 94 (2018) 124–140, https://doi.org/10.1016/j.ijepes.2017.06.035.

[3] A.T. Langeroudi, M.M.A. Abdelaziz, Preventative high impedance fault detection using distribution system state estimation, Electr. Power Syst. Res. 186 (2020), 106394, https://doi.org/10.1016/j.epsr.2020.106394.

[4] M.J.S. Ramos, M. Resener, A.S. Bretas, D.P. Bernardon, R.C. Leborgne, Physics based analytical model for high impedance fault location in distribution networks, Electr. Power Syst. Res. 188 (2020), 106577, https://doi.org/10.1016/j.epsr.2020.106577.

[5] S. Gautam, S.M. Brahma, Detection of high impedance fault in power distribution systems using mathematical morphology, IEEE Trans. Power Deliv. 28 (2013) 1226–1234, https://doi.org/10.1109/tpwrs.2012.2215630.

[6] M. Pignati, L. Zanni, P. Romano, R. Cherkaoui, M. Paolone, Fault detection and faulted line identification in active distribution networks using synchrophasors based real-time state estimation, IEEE Trans. Power Deliv. 32 (2017) 381–392, https://doi.org/10.1109/TPWRD.2016.2545923.

[7] E.M. Lima, C.M.S. Junqueira, N.S.D Brito, B.A. Souza, R.A. Coelho, H.G.M. S. Medeiros, High impedance fault detection method based on the short-time Fourier transform, IET Gener. Transm. Distr. 12 (2018) 2577–2584, https://doi.org/10.1049/iet-gtd.2018.0093.

[8] M.Y. Suliman, M.T. Ghazal, Detection of high impedance fault in distribution network using fuzzy logic control, in: Proceedings of the 2nd International Conference on Electrical, Communication, Computer, Power and Control Engineering, 2019, pp. 103–108, https://doi.org/10.1109/ICECCPCE46549.2019.203756.

[9] A. Ghaderi, H.L. Ginn, H.A. Mohammadpour, High impedance fault detection: a review, Electr. Power Syst. Res. 143 (2017) 376–388, https://doi.org/10.1016/j.epsr.2016.10.021.

[10] M. Biswal, S. Ghore, O.P. Malik, R.C. Bansal, Development of time-frequency based approach to detect high impedance fault in an inverter interfaced distribution system, IEEE Trans. Power Deliv. (2021), https://doi.org/10.1109/tpwrd.2021.3049572.
[11] M.J.S. Ramos, A.S. Bretas, D.P. Bernardo, L.L. Pfitscher, Distribution networks HIF location: a frequency domain system model and WLS parameter estimation approach, Electr. Power Syst. Res. 146 (2017) 170–176, https://doi.org/10.1016/j.epsr.2017.01.030.
[12] X. Wang, X.Wei J.Gao, G. Song, L. Wu, J. Liu, Z. Zeng, M. Kheshti, High impedance fault detection method based on variational mode decomposition and Teager–Kaiser energy operators for distribution network, IEEE Trans. Smart Grid 10 (2016) 6041–6054, https://doi.org/10.1109/tsg.2019.2895634.
[13] J. Nunes, A. Bretas, N. Bretas, A. Herrera-Orozco, L. Iurinic, Distribution systems high impedance fault location: a spectral domain model considering parametric error processing, Int. J. Electr. Power Energy Syst. 109 (2019) 227–241, https://doi.org/10.1016/j.ijepes.2019.02.012.
[14] C. Gonzalez, J. Tant, J.G. Germain, T. De Rybel, J. Driesen, Directional, high-impedance fault detection in isolated neutral distribution grids, IEEE Trans. Power Deliv. 33 (2018) 2474–2483, https://doi.org/10.1109/TPWRD.2018.2808428.
[15] S.H. Mortazavi, Z. Moravej, S.M. Shahrtash, A searching based method for locating high impedance arcing fault in distribution network, IEEE Trans. Power Deliv. 34 (2019) 438–447, https://doi.org/10.1109/TPWRD.2018.2874879.
[16] W.C. Santos, F.V. Lopes, N.S.D. Brito, B.A. Souza, High-impedance fault identification on distribution networks, IEEE Trans. Power Deliv. 32 (2017) 23–32, https://doi.org/10.1109/TPWRD.2016.2548942.
[17] S. Silva, P. Costa, M. Gouvea, A. Lacerda, F. Alves, D. Leite, High impedance fault detection in power distribution systems using wavelet transform and evolving neural network, Electr. Power Syst. Res. 154 (2018) 474–483, https://doi.org/10.1016/j.epsr.2017.08.039.
[18] A. Ghaderi, H.A. Mohammadpour, H.L. Ginn, Y.J. Shin, High-impedance fault detection in the distribution network using the time-frequency-based algorithm, IEEE Trans. Power Deliv. 30 (2014) 1260–1268, https://doi.org/10.1109/tpwrd.2014.2361207.
[19] S. Silva, P. Costa, M. Santana, D. Leite, Evolving neuro-fuzzy network for real-time high impedance fault detection and classification, Neural Comput. Appl. 32 (2020) 7597–7610, https://doi.org/10.1007/s00521-018-3789-2.
[20] B.K. Chaitanya, A. Yadav, M. Pazoki, An intelligent detection of high-impedance faults for distribution lines integrated with distributed generators, IEEE Syst. J. 14 (2019) 870–879, https://doi.org/10.1109/jsyst.2019.2911529.
[21] M. Mishra, P.K. Rout, Detection and classification of micro-grid faults based on HHT and machine learning techniques, IET Gener. Transm. Distrib. 12 (2018) 388–397, https://doi.org/10.1049/iet-gtd.2017.0502.
[22] P.E. Farias, A.P. de Morais, J.P. Rossini, G. Cardoso, Non-linear high impedance fault distance estimation in power distribution systems: a continually online-trained neural network approach, Elect. Power Syst. Res. 157 (2018) 20–28, https://doi.org/10.1016/j.epsr.2017.11.018.
[23] M. Dhimish, V. Holmes, B. Mehrdadi, M. Dales, Comparing Mamdani Sugeno fuzzy logic and RBF ANN network for PV fault detection, Renew. Energy 117 (2018) 257–274, https://doi.org/10.1016/j.renene.2017.10.066.
[24] R. Azim, F. Li, Y. Xue, M. Starke, H. Wang, An islanding detection methodology combining decision trees and Sandia frequency shift for inverter-based distributed generations, IET Gener. Transm. Distrib. 11 (2017) 4104–4113, https://doi.org/10.1049/iet-gtd.2016.1617.
[25] MATLAB. version (R2016a). Natick, The MathWorks Inc, Massachusetts, 2016.
[26] M. Michalik, W. Rebizant, M. Lukowicz, S.J. Lee, S.H. Kang, High impedance fault detection in distribution networks with use of wavelet-based algorithm, IEEE Trans. Power Deliv. 21 (2006) 1793–1802, https://doi.org/10.1109/tpwrd.2006.874581.
[27] A.I. Megahed, A. Monem Moussa, H.B. Elrefaie, Y.M. Marghany, Selection of a suitable mother wavelet for analyzing power system fault transients, in: Proceedings of the IEEE Power and Energy Society General Meeting - Conversion and Delivery of Electrical Energy in the 21st Century, 2008, pp. 1–7, https://doi.org/10.1109/PES.2008.4596367.
[28] K. Sekar, N.K. Mohanty, A fuzzy rule base approach for high impedance fault detection in distribution system using Morphology Gradient filter, J. King Saud Univ. Eng. Sci. 32 (2020) 177–185, https://doi.org/10.1016/j.jksues.2018.12.001.
[29] M. Sarlak, S.M. Shahrtash, D.A. Khaburi, Design and implementation of a systematically tunable high impedance fault relay, ISA Trans. 49 (2010) 358–368, https://doi.org/10.1016/j.isatra.2010.03.011.